ingegneria sismica
International Journal of Earthquake Engineering
Anno XLIII - Num. 2 - 2026

A Study on an Early Warning System for Identifying Illegal Dumping of Construction Waste and Debris Near Power Construction Sites Based on Remote Sensing Images

Zilong Zhou[1], *Tingming Ye*[1,*], *Wenliang Lin*[2], *Peng Li*[1], *Yulong Lyu*[1] *and Jianmin Bai*[2]

[1] Jibei Electric Power Research Institute, State Grid Jibei Electric Power Co., Ltd., Beijing 100045, China
[2] State Grid Jibei Electric Power Co., Ltd. Zhangjiakou Power Supply Company, Zhangjiakou, Hebei, China

SUMMARY: *For solving the difficult problems that relate to the unlawful pouring of building rubbish and fragments close to electric power construction places—including dispersed objects, broken dividing lines, big mixing with open building places and lawful treating areas, and slow reacting speeds in traditional inspections—this article puts forward one recognition and early warning system which is based on remote sensing. This system has built a multi-source data arrangement frame which includes an engineering restriction layer, a time remote sensing layer, and a high-resolution detailed check layer. At first, it carries out the definition of the candidate search region on the basis of power line corridors, tower foundations, substation expansion areas, construction access roads, and already approved disposal places. It then uses constraint-guided spatiotemporal boundary refinement networks to perform anomaly screening, three-branch feature coding, and target boundary restoration.Finally, a hierarchical early warning mechanism is established by integrating criteria such as persistence, expansion, deviation from legality, and environmental sensitivity. Results show that CSBR-Net achieves a peak F1 score of 89.2% on the overall test set, with an average F1 of 89.6% across scenarios, and maintains an 87.4% recognition rate even under wet surface conditions; the latency of the complete model is 43.0 ms per image, representing improvements of 4.6 and 7.3 percentage points over the optical baseline in F1 and mIoU, respectively. Typical examples have shown that risk numerical values can pass the alarm and attention critical points before the goal region obviously enlarges, hence giving early notification for on-the-spot checking. This research therefore points out that putting engineering law limit requirements, time change data, and fine divided boundary description into one single decision-making chain can effectively promote the stability and deployable ability of illegal soil and waste dumping inspection and early warning systems that lie near electric power construction projects.*

KEYWORDS: *remote sensing imagery; power construction; dumped soil and debris; illegal dumping identification; early warning system*

1 Introduction

Electric power building works have the features of long power transfer line paths, scattered building positions, many different influenced zones, and fast stage changes. Foundation digging, access way building, stringing yard arranging, electric substation enlarging, and temporary

*ye.tingming@jibei.sgcc.com.cn
https://doi.org/10.65102/is2026753
Published: 30 April, 2026

stockpile setting up can change surface exposure in a short time period and produce continuous earth work and rock carrying needs that go outside project boundaries. If dug-out soil and construction garbage are not carried to approved processing places but are instead temporarily unloaded along construction access roads, valley side slopes, river bank slopes, or empty lands in villages and towns, this therefore often brings about spilling beyond project borders, increased slope exposure, blocked vegetation growth recovery, and dangers of secondary erosion. A summary of environment dangers in the building period of electric power transmission and distribution projects shows that current regulation systems still have no effective real-time watch and feedback systems, therefore it is hard to quickly count and find out early-period ecological dangers. Investigation of construction waste disposal places also demonstrates that confirming interference boundaries, recording alterations in waste quantities, and obtaining soil and water protection measures demand the combination of remote sensing, GIS, and position data; Only the spot checking work by itself is not able to finish the work of entire, from start to end supervision [1, 2].

Under this background, remote sensing image gives an expandable space observation tool for monitoring soil and waste placement places around electric power construction projects. Reviews which concentrate on solid waste and dumping situations generally hold the view that remote sensing can cover large zones with low expense and, by means of repeated observations, it supports a continuous procedure that goes from detection and screening to dynamic tracking [3-5]. Studies which are based on deep learning about global distribution of dumping places further prove that the space distribution of garbage is obviously connected with land surface shape, human behaviors, and around reachability. Information which is about morphology, texture, road neighbor situation, and land cover combinations inside satellite picture data can together give support to the work of candidate site identification [6]. To business situations like electric power construction—that contain "linear project + multi-spot building + dynamic interference"—the worth of remote sensing is not to replace on-spot check, but it is firstly to reduce the scope of spatial positions which need first check from a big region.

Existing research has advanced the identification of illegal dumping at both the data and model levels.Regarding open data, AerialWaste provides 10,434 landfill detection datasets derived from multi-source ultra-high-resolution imagery, while CWLD has constructed 3,653 high-resolution samples with pixel-level annotations specifically for construction waste landfills, providing a transferable data foundation for scene classification, object detection, and semantic segmentation [7, 8]. In terms of applied methods, Yong et al. implemented the detection of illegal construction demolition waste landfills from a computer vision perspective, Sánchez-Fernández et al. utilized topographic anomalies in LiDAR DEMs to characterize illegal construction waste dumping, while Zhang and Ma's CascadeDumpNet and Gibellini et al.'s remote sensing detection pipeline for environmental regulation demonstrate that combining high-resolution imagery with contextual modeling and staged screening can effectively reduce false positives caused by irrelevant bare ground [9-12]. Furthermore, the TSNET proposed by Yu et al. incorporates instance segmentation into solid waste recognition, indicating that detailed representations of boundaries and morphology are emerging as a new direction for improvement [13].

But, when we directly put already obtained outcomes into the situations that are around electric power construction projects, we still meet four obvious difficult problems. Firstly, the objects of this research have differences. Existing work primarily focuses on municipal waste, open dumpsites, or urban construction debris, where targets typically manifest as area-based sites; in contrast, abnormal soil and debris dumping in power construction more frequently occurs in a dispersed manner along transmission line corridors, access roads, tower clusters, and temporary construction sites, characterized by small scales, fragmented boundaries, and

rapid movement.Second, legal compliance information is not integrated into the core identification process. Most remote sensing methods directly classify targets based on image appearance without incorporating project boundaries, approved disposal zones, temporary backfill areas, and surrounding sensitive objects into the same classification framework. Consequently, areas that "appear to be waste" may not necessarily be in violation of regulations. Third, the temporal dimension is underutilized.Existing research places greater emphasis on single-period identification or static extraction, failing to adequately address early warning questions such as "when it appeared, whether it persists, whether it is expanding rapidly, and whether it is near sensitive sites." Fourth, there remains a disconnect between identification results and disposal priorities. For regulatory authorities overseeing the construction phase, identification results only possess direct disposal value when linked to temporal evolution and project constraints.

According to these problems, this paper reduces its research target to: build an early warning system that can identify illegal dumping of construction waste which is near power construction places. This system has already put together engineering legitimacy limiting conditions, space-time changing messages, and high-resolution boundary distinguishing abilities, therefore thus it can realize continuous processing which starts from the finding of candidate abnormal things, and detailed distinguishing, and finally arrives at multi-level risk warnings.

For the completion of this target, the present paper carries out the following work items. Firstly, with a focus on engineering objects which include tower foundations, access roads, tensioning working sites, substation expansion regions, and approved waste disposal sites, we have established a compliance search domain and a sampling organization method for the nearby areas of electric power construction projects, which thus makes it possible that engineering disturbances and illegal dumping can be distinguished under identical spatial constraints. Second, we put forward a constraint-guided space-time boundary fine-modification framework that integrates multi-time change hints, geometry validity masks, and high-resolution texture characteristics to strengthen the distinguishing of small-scale, broken, and heavily covered waste dumping blocks. Third, according to the results of identification, we introduce factors including persistence, expansion, environmental sensitivity to build a layered early warning mechanism, therefore providing a usable technical route for ecological supervision and quick response in the construction period of power projects.

2 Methods

2.1 Multi-source Remote Sensing Data Organization and Compliant Search-Domain Construction

For facing the regulation demands of supervising unlawful discard of building rubbish and dreg around electric power construction places, this research sets up a multi-source data system which includes an engineering restriction layer, a time sequence remote sensing layer, and a high-resolution detailed check layer. The engineering restriction level contains space objects such as power line paths, tower base grounds, tension working places, power station expanding regions, building entering roads, permitted throwing places, legal temporary holding zones, and also around water channels, living areas, and sensitive sloped lands, which are utilized to delimit the observing range which directly connects with engineering activities; The time remote sensing level mainly uses Sentinel-2 optical image, Sentinel-1 radar image, and Harmonized Landsat and Sentinel-2 data to continuously follow the expansion of bare soil appearing, vegetation becoming bad, and surface being disturbed; the high-resolution checking level uses sub-meter optical pictures to check the borderlines and amend the categorization of

selected abnormal regions. For the purpose of illustrating the organizational relation among engineering legitimacy restrictions, multi-source observation hierarchies, and sample establishment, please refer to Figure 1.

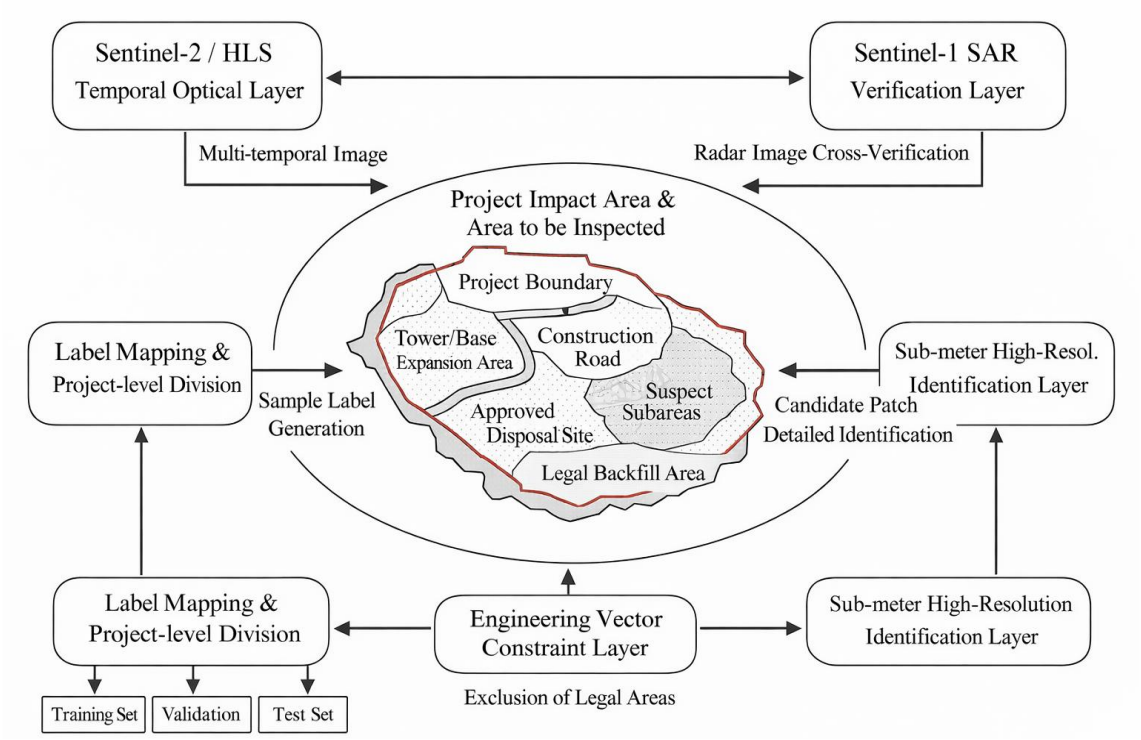

Figure 1: Diagram of multi-source data organization and sample construction mechanisms around power construction sites.

Existing research indicates that the key challenges in environmental risk early warning during the construction phase of power transmission and distribution projects lie in insufficient continuous monitoring, spatial feedback lag, and inadequate utilization of project constraint information; accordingly, monitoring of construction waste disposal also relies more on the coordinated integration of remote sensing, GIS, and location data to support disturbance boundary identification, waste disposal site classification, and continuous tracking [14].

As for the arrangement of objects, this paper does not carry out a global searching on the whole image directly. On the contrary, it firstly builds the influence scope of the project according to project borders, construction access paths, tower base distributions, and substation expanding borders. It then from this area excludes approved disposal places, lawfully designated backfill regions, and registered temporary storage sections to form a candidate search scope which needs concentrated screening. This method firstly utilizes engineering restriction conditions to sift out irrelevant background information, hence decreasing wrong positive results brought by natural bare earth, turned plow land, and common construction interferences. At the same time, it gives a clear legitimacy reference for following recognition results, therefore enabling the model to make distinction between "visually alike but conforming" stockpile places and abnormal patches that bring real compliance risks. Because power construction usually has both point-type construction places and line-type construction passages, therefore the candidate searching region is dynamically pieced together according to engineering objects, it does not use a simple cutting method with fixed windows. The composition of multi-source remote sensing and engineering restriction data layers is displayed in Table 1.

Table 1: Configuration of Multi-source Remote Sensing and Engineering Constraint Data Layers

Data Layer	Main Source	Typical Spatial Resolution	Temporal Features	Role in the System
Temporal Optical Screening Layer	Sentinel-2 MSI L2A	10–20 m	5 d	Construct clues for bare soil, vegetation, and surface exposure changes
Temporal Radar Verification Layer	Sentinel-1 C-band SAR	~10 m	6 d repeat-pass	Suppress cloud and fog effects, supplement roughness and moisture change information
Dense Temporal Synthesis Layer	HLS	30 m	2–3 d	Establish stable temporal baselines and continuous anomaly sequences
Fine Identification Layer	Sub-meter High-Resolution Optical Imagery	0.5–0.8 m	Organized by acquisition period	Provide a basis for high-precision labeling and boundary extraction
Engineering Constraint Layer	Engineering red lines, approval disposal areas, tower bases, access roads, water systems, settlements, slope-sensitive areas	Vector	Updated with engineering changes	Provide basis for legality constraints and risk sensitivity calculations

In terms of data processing, this study adopts a two-tiered organizational strategy of "sequential screening first, followed by high-resolution confirmation." First, a background baseline is established using pre-construction imagery from the same season to mitigate false changes caused by seasonal bare ground, short-term wet soil, shadows, and fog; subsequently, persistent or gradually expanding disturbance areas are extracted from continuous-phase imagery and cropped into candidate patches;Finally, the candidate patches are fed into a high-resolution verification layer, where clearer texture, geometric, and boundary information is used to confirm the targets. Relevant reviews indicate that the stability of remote sensing monitoring for solid waste relies heavily on multi-temporal information, data source harmonization, and contextual constraints, while multi-temporal products with a unified reflectance band are better suited for continuous screening tasks across time and space.

Sample label work uses a five-category system, which corresponds to unlawful soil and rubbish tipping, lawful processing or temporary piling up, building-exposed land, material heaps, and natural uncovered ground and other background parts. This classification does not aim to perfect operation categories, but on the contrary to keep the most easily mixed neighboring classes, therefore enabling follow-up models to study distinctions among unlawful dumping, lawful work zones, and ordinary naked land within one unifying classification framework. Besides samples that are produced by projects, this paper uses AerialWaste and CWLD as outside supplementary sources to solve hard samples in open dumping and

construction waste situations, hence strengthening the model's adaptability for complex textures and multi-scale boundaries. When we carry out partitioning of the data, the training, validation, and test sets are divided through engineering project method instead of through random tiles. Samples which come from different time stages of the identical project have not been mixed among sets, therefore to avoid the overestimation of performance which is caused by spatial leakage. Through this arrangement, a clear corresponding relationship was built among the data sources, candidate search scopes, and marking system, hence providing a unified input base for the constraint-guided time-space recognition model that is introduced in the following section.

2.2 Constraint-guided spatiotemporal boundary refinement network

Existing remote sensing methods for solid waste recognition have evolved from multi-scale context-fusion detection [15], anchor-based aerial object detection [16], keypoint-guided urban solid waste detection [17], and scene classification [18], to change detection modeling [19-22] and pre-training strategies tailored for the remote sensing domain [23, 24]. However, the great majority of these methods put focus on judging "whether an object has existence in the image," thus lacking a clear expression of engineering-approved boundary lines and time-based continuance. In order to deal with the features that small pieces, broken borders, serious sheltering, and stage movement exist together around electric power construction places, this paper puts forward the Constraint-guided Spatiotemporal Border Refinement Network (CSBR-Net). This network is composed by a candidate abnormal screening module, a three-branch feature coding module, and a boundary refinement decoding module: the first stage quickly reduces the search range inside the target region; the second stage carries out instance-level identification and edge adjustment on high-resolution candidate blocks; the third stage, therefore, combines the result outputs from each instance with the engineering restriction level, hence forming the follow-up early warning objects. For giving explanation to the coupling relation among candidate anomaly screening, three-branch feature encoding, and boundary refinement decoding, one may look at Figure 2.

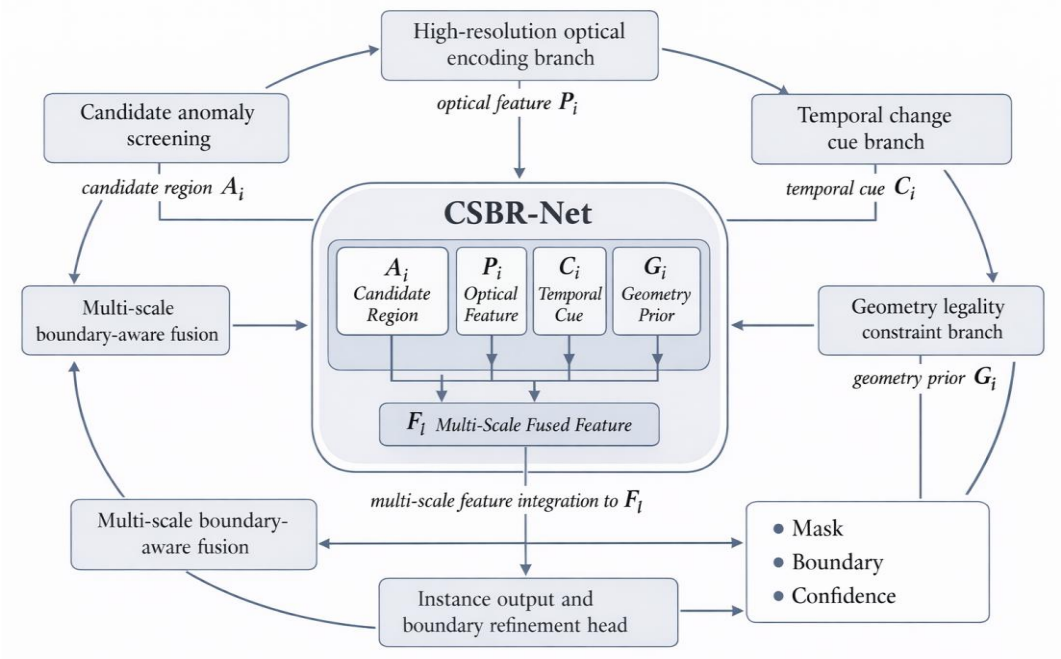

Figure 2: Coupled Recognition Mechanism Diagram for Legality Constraints-Spatio-Temporal Changes-Boundary Refinement.

Figure 2 centers on CSBR-Net, integrating candidate search area compression, temporal variation characterization, geometric validity constraint embedding, and high-resolution boundary refinement into a single recognition framework.In the first stage, candidate screening is performed using temporal anomaly responses within the inspection area defined by engineering constraints, eliminating stable bare ground, short-term disturbances, and irrelevant objects from the broader background to reduce the computational burden of subsequent high-resolution recognition;In the second stage, candidate tiles are simultaneously fed into the optical branch, the change cue branch, and the geometric constraint branch to extract texture boundaries, continuous change information, and structural features related to adjacency with valid areas, roads, and tower bases, respectively;In the third stage, through multi-scale fusion and boundary refinement, the system jointly outputs target masks and boundary probability maps, enabling the model to handle complex morphologies-such as scattered stockpiles, elongated overflows, and fragmented boundaries at the base of slopes-more stably.

Candidate anomaly screening is performed within the inspection area at the pixel block or small patch level. For the th candidate unit (i), a temporal anomaly scoreA_i is constructed as shown in Equation (1).

$$A_i = \omega_1 \Delta \widetilde{BSI}_i + \omega_2 \Delta \widetilde{NDBI}_i + \omega_3 (1 - \Delta \widetilde{NDVI}_i) + \omega_4 \Delta \widetilde{\sigma^0}_i + \omega_5 \Delta \widetilde{H}_i \quad (1)$$

Here, A_i represents the composite anomaly score of the i th candidate cell; $\Delta \widetilde{BSI}_i$, $\Delta \widetilde{NDBI}_i$, and $\Delta \widetilde{NDVI}_i$ represent the normalized temporal variations of the bare soil index, built-up area index, and vegetation index, respectively; $\Delta \widetilde{\sigma^0}_i$ represents the SAR backscatter variation; $\Delta \widetilde{H}_i$ denotes texture entropy changes; $\omega_1 \sim \omega_5$ are normalized weights that satisfy $\sum \omega k = 1$. When A_i exceeds the candidate threshold and remains high across two consecutive time slices, the area is sent to the fine-grained identification stage. The purpose of this approach is to first use low-cost temporal information to exclude large areas of stable background, and then concentrate high-resolution computations on areas truly worthy of review.

Upon entering the second stage, the$i$ th candidate block is simultaneously fed into the optical branch, the change cue branch, and the geometric constraint branch.The optical branch extracts color, texture, and morphological boundaries from high-resolution imagery; the change cue branch encodes the change intensity map generated by the temporal screening stage C_i; and the geometric constraint branch embeds valid region masks, distance fields, and road/tower base proximity relationships to obtain a constraint mapG_i. At the$l$ layer, the multi-branch fusion features are denoted as F_l, as shown in Equation (2).

$$F_l = \phi_l\left(E_l^o(P_i) \oplus E_l^c(C_i) \oplus E_l^g(G_i)\right) \quad (2)$$

Here, P_i represents the i th candidate high-resolution tile; $E_l^o(\cdot)$, $E_l^c(\cdot)$, and $E_l^g(\cdot)$ denote the optical, variation, and geometric encoding results of the l th layer, respectively; $\oplus$ denotes channel concatenation; and $\phi_l(\cdot)$ denotes the boundary-aware fusion operator. This design does not treat geometric constraints as post-processing conditions applied to the recognition results but instead incorporates them directly into the encoding at the feature layer, enabling the model to obtain more stable classification criteria in scenarios such as boundary spillover, road adjacency, and edge-hugging within valid regions. The decoding stage employs a combination of layer-wise upsampling and a boundary refinement head to jointly output the target mask and boundary probability map, thereby enhancing the model's ability to represent scattered dumping, elongated overflows, and fragmented boundaries at the foot of slopes.

During training, a joint loss is used to constrain classification, masking, boundaries, and temporal consistency, as shown in Equation (3).

$$L = \lambda_1 L_{cls} + \lambda_2 L_{dice} + \lambda_3 L_{bnd} + \lambda_4 L_{con} \tag{3}$$

Here, L represents the total loss; L_{cls} denotes the classification loss for the illegal waste dumping class; L_{dice} denotes the segmentation loss for the mask; L_{bnd} denotes the boundary refinement loss; L_{con} denotes the temporal consistency loss; and λ_1 to λ_4 are weight coefficients.To enhance cross-scenario generalization, the parameters of the backbone network are initially initialized using pre-trained weights from remote sensing data, and hard negative sample resampling is introduced during training to ensure that highly confounding samples-such as construction bare ground, material stockpiles, and legally permitted temporary storage sites-are repeatedly learned throughout the iterative process.

2.3 Warning Scoring Strategy and Experimental Protocol

After the recognition results are got out, this paper will not give out an alert according to merely one detection result; on the contrary, it gathers together space objects, time continuity, and engineering constraints into an object-level risk score. For the j th alert object, the comprehensive risk scoreR_j is defined, as shown in Equation (4).

$$R_j = \alpha p_j + \beta e_j + \gamma t_j + \delta h_j + \eta d_j \tag{4a}$$

$$\alpha + \beta + \gamma + \delta + \eta = 1 \tag{4b}$$

where R_j denotes the risk score of the$j$ th object;p_j denotes the identification confidence; e_j denotes the area expansion rate; t_j denotes the persistence score; h_j denotes the environmental sensitivity score; d_j denotes the compliance deviation; α, β, γ, δ, andη are normalized weights. h_j is calculated based on the spatial relationship between the object and watercourses, residential areas, slope-sensitive zones, and drainage channels, while d_j is determined by the overlap between the object and the approved absorption area, the shortest distance, and whether the object extends beyond the project's permitted disturbance boundary. Based on the magnitude of R_j and trends across consecutive time slices, the system establishes three warning levels: "Alert," "Monitor," and "Action." When an object exhibits a single-period anomaly and is located near a legal operational zone, it remains at the Alert level; when the anomaly persists or its area shows significant growth, it is elevated to the Monitor level; when the anomaly is located in an illegal area and increases for two consecutive periods, it enters the Action level, and a verification task is pushed.

The experimental protocol combines project-level segmentation with cross-scenario validation to avoid spatial information leakage caused by random tile segmentation. The training, validation, and test sets are divided according to engineering projects rather than randomly partitioned by tiles; different time slices within the same project are not mixed across sets. The comparison methods are divided into three groups: first, object detection methods represented by CascadeDumpNet, SWDet, and LKN-ME; second, segmentation or instance segmentation methods represented by TSNET and MCFN; and third, lightweight deep learning baselines for rapid identification of high-resolution aerial imagery [25]. Evaluation metrics include Precision, Recall, F1, mAP@0.5, mIoU, and single-image inference time; for early warning tasks, object-level hit rate, false alarm rate, and average lead time are additionally calculated. Furthermore, experiments were conducted under various scenarios-including

mountainous/hilly/plains terrain, power line corridors/station site expansion, dry season/rainy season, and different resolution conditions to verify the system's adaptability to variations in terrain, season, and project type. The aforementioned setup ensures that the entire chain-from engineering constraints and anomaly detection to detailed identification and operational early warning-is evaluated under the same protocol. Based on this, the following sections will compare overall performance, module contributions, and performance in typical scenarios. To illustrate the closed-loop relationship between the experimental protocol, risk scoring, and graded response, see Figure 3.

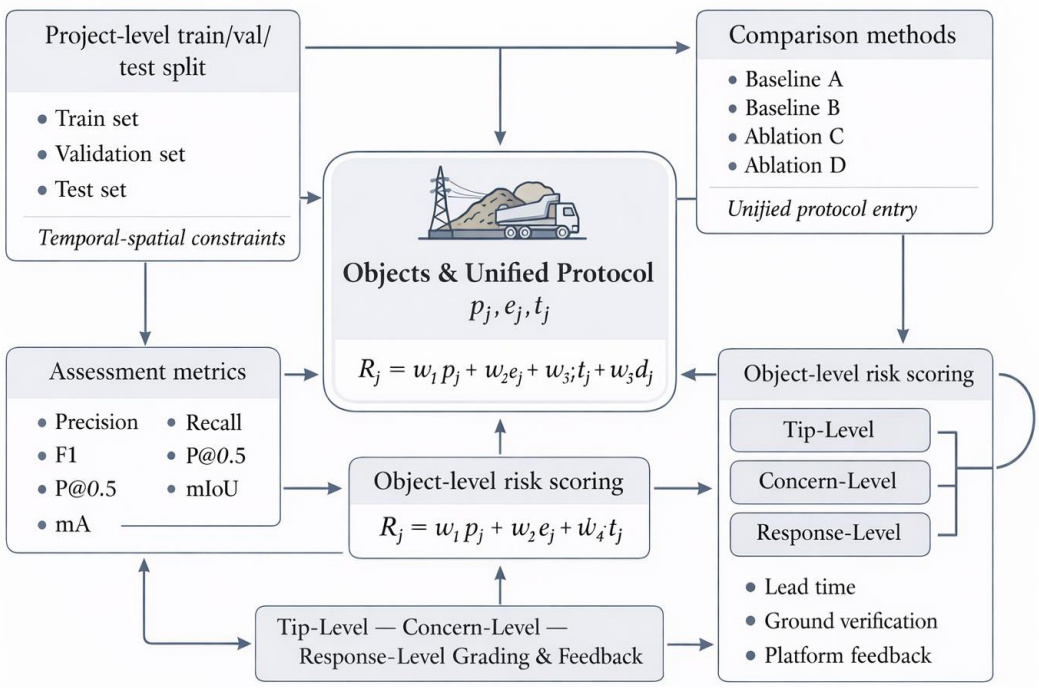

Figure 3: Diagram of Alert Grading and Experimental Protocol.

3 Results and Discussion

3.1 Overall Detection Performance and Cross-Scene Robustness

In this section, we first discuss whether the system can stably tell apart illegal soil and rubble dumping from visual similar ground changes in complicated engineering situations, and furthermore we research whether this recognizing ability keeps unchanged across different landforms, engineering categories, and surface situations. For making the explanation of outcomes keep based on actual world objects, we at first compare the target shape features with the main interference sources in the testing data set, which is displayed in Figure 4.

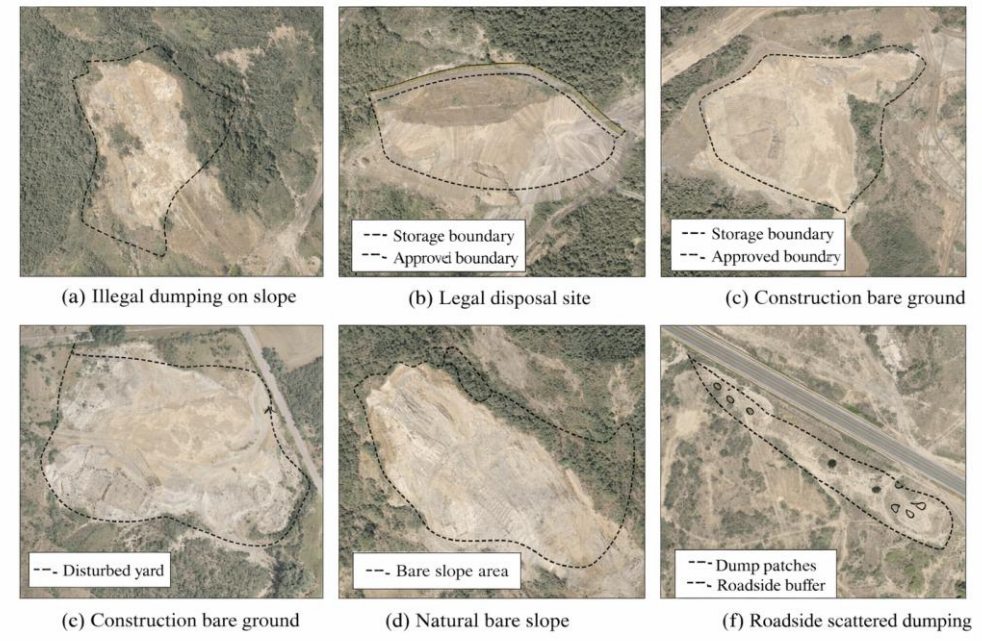

Figure 4: Representative illegal-dumping targets and high-confusion background scenes.

Figure 4 presents typical anomalous targets alongside high-confusion background scenes in a single set of images. Figure 4(a) depicts illegal waste dumping on a slope, characterized by irregular boundaries but a contiguous main body, with the outer edges extending outward along the slope; Figure 4(f) corresponds to scattered piles of waste alongside a road, where the target scale is smaller and exhibits a discrete, multi-patch distribution.In contrast, the legal disposal site in Figure 4(b), although also characterized by bright bare soil and a closed contour, is enclosed within approved boundaries; the construction-exposed ground in Figure 4(c) and the natural bare slope in Figure 4(e) both exhibit strong bare-ground textures and irregular boundaries, making them prone to visual confusion with illegal dumping;In contrast, the material stockpile in Figure 4(d) exhibits a more distinct, regular geometric shape. This set of figures demonstrates that texture or morphological information alone is insufficient for reliable classification; truly effective identification requires the simultaneous use of legality constraints, temporal variation cues, and boundary refinement results. After completing the scene-level comparison, we further evaluate the classification performance of different methods on the entire test set, as shown in Figure 5.

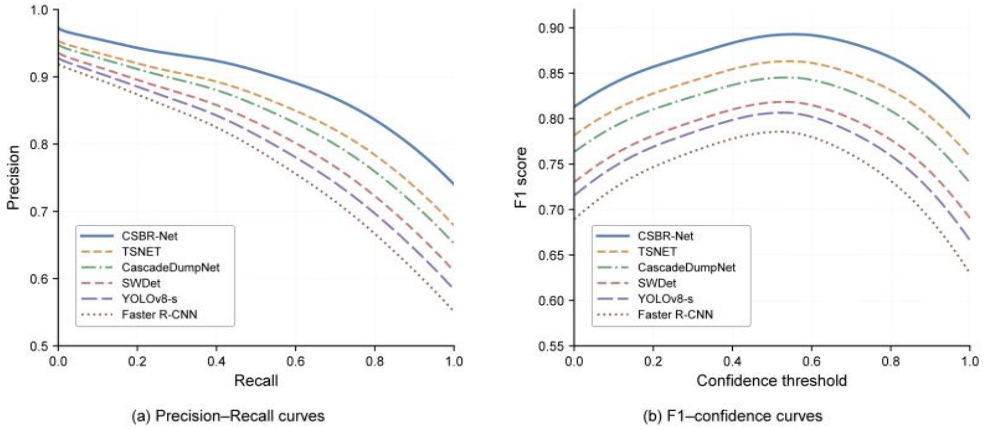

Figure 5: Precision-Recall and F1-confidence curves of different detection methods.

Figure 5(a) gives out the Precision-Recall curves. The curve which belongs to CSBR-Net holds an envelop-shaped advantage in the whole scope of recall; When the recall reaches 0.80, the precision still holds 86.7%, which is significantly higher than the 79.6% of TSNET, the 77.0% of CascadeDumpNet, the 73.4% of SWDet, the 70.6% of YOLOv8-s and the 67.2% of Faster R-CNN. This shows that when the recall condition is high, the method put forward by us can give more stable inhibition to false positive results. Figure 5(b) in addition gives the F1-confidence curves. CSBR-Net obtains its highest F1 value when the confidence threshold is about 0.58-0.60, therefore reaching the peak at 89.2%; the peak F1 numerical values for TSNET, CascadeDumpNet, SWDet, YOLOv8-s, and Faster R-CNN are about 86.2%, 84.4%, 81.7%, 80.5%, and 78.4%, each one separately. In addition, CSBR-Net keeps a high F1 score in a broad threshold scope of 0.40-0.75, which shows the model has no sensitivity to threshold settings, hence therefore it provides better engineering adaptability during combination with early warning systems. Besides the whole accuracy, we also have the necessity to discuss the model's steadiness in various engineering situations, as what is displayed in Figure 6.

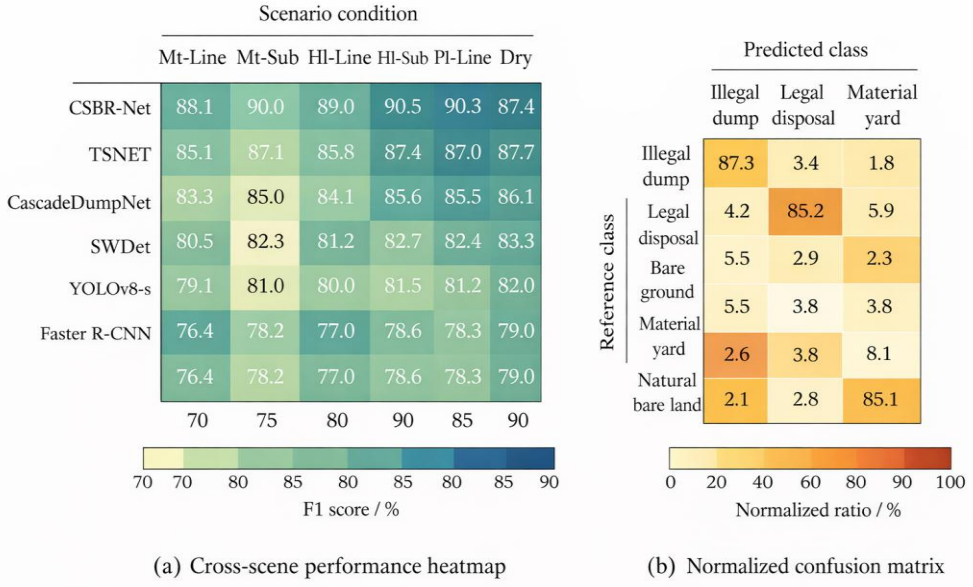

Figure 6: Cross-scene performance heatmap and normalized confusion matrix of CSBR-Net.

Figure 6(a) gives out the cross-scene F1 heat distribution graph, in which Mt-Line, Mt-Sub, Hl-Line, Hl-Sub, Pl-Line, Pl-Sub, Dry, and Wet separately correspond to mountain area power transmission lines, mountain area transformer station places, hill area power transmission lines, hill area transformer station places, flat land power transmission lines, flat land transformer station places, dry surface situations, and wet surface situations. CSBR-Net obtains F1 value scores of 88.1%, 90.0%, 89.0%, 90.5%, 90.3%, 91.0%, 90.4%, and 87.4% in the eight different scenarios, with an average value of 89.6%, which is higher than the average value of all other baseline methods. Figure 6(b) gives out the normalized confusion matrix that belongs to CSBR-Net, on its diagonal, the classification rates of five target classes are 87.3%, 85.2%, 83.0%, 81.3%, and 85.1%, separately. The main confusion is gathered together in the categories which relate to uncovered land. To speak specifically, 7.2 percent of material stock piles were wrongly divided into the type of bare ground, and 6.6 percent of natural bare ground was wrongly classified into the type of bare ground. This shows that the present residual error mainly comes from extremely alike empty land background, hence confusion directly between unlawful waste stacking sites and regular handling zones has thus been greatly decreased.

A comprehensive analysis of Figures 4 to 6 reveals that the advantages of the method

proposed in this paper are not limited to improvements in a single metric but are further demonstrated by its stable response to disturbances in complex scenarios. In environments surrounding power construction projects-where point-like construction sites, linear corridors, and multiple types of bare land coexist-only by integrating project boundaries, continuous changes, and fine-grained boundary representations into a single classification chain can the model achieve a more balanced result between high recall and low false positive rates.

3.2 Module Contribution, Accuracy-Efficiency Trade-off, and Temporal Warning Capability

After verifying the overall performance, this section further addresses two questions: first, what each module contributes individually; and second, whether the recognition results can be successfully converted into early warning outputs with a time lead. The former concerns the necessity of the model design, while the latter concerns whether the system possesses practical regulatory value, as shown in Figures 7 and 8.

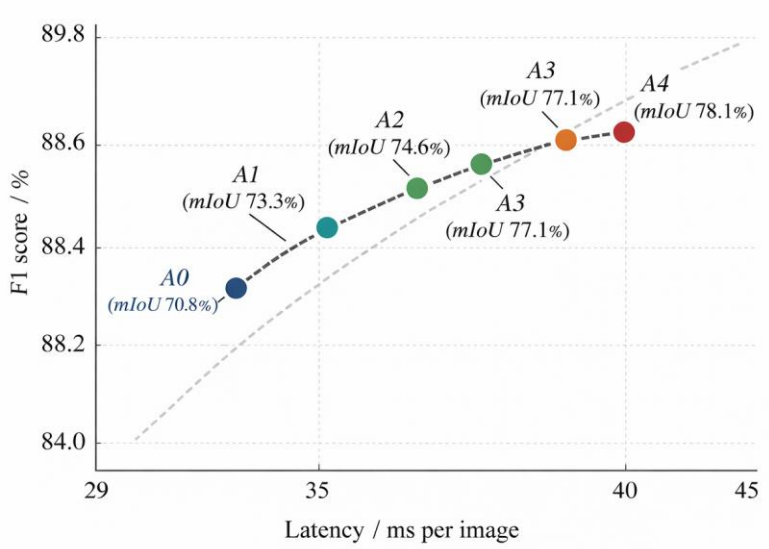

Figure 7: Ablation-based accuracy-efficiency trade-off of different model variants.

In Figure 7, F1, mIoU, and single-image time delay of five ablation changing types are compared in one coordinate plane. A0 is the baseline model using only the optical branch, with an F1 of 84.6%, mIoU of 70.8%, and single-image latency of 31.0 ms.After incorporating temporal cues, A1's F1 score improves to 86.7%, mIoU to 73.3%, and latency increases to 35.0 ms, indicating that temporal anomaly cues primarily enhance the quality of candidate screening for determining "whether further evaluation is warranted."Upon further incorporation of geometric validity constraints, A2 achieved an F1 score of 87.9%, an mIoU of 74.6%, and a latency of 37.0 ms. This improvement was primarily reflected in false positive suppression, particularly in the more stable differentiation between valid absorption zones, construction-exposed areas, and general construction disturbances.After adding the boundary refinement head to A3, the F1 score further improved to 88.6% and the mIoU to 77.1%, indicating that boundary learning contributes more directly to scenarios involving elongated spillovers, fragmented slope bases, and scattered waste piles.The complete model A4 achieves an F1 score of 89.2% and an mIoU of 78.1%, for each image, it possesses a latency that is 43.0 ms. When we compare with A0, this situation expresses that there are 4.6 percentage points and 7.3 percentage points promotion respectively, while the total time delay has a rise of only 12.0 ms. The linear relation that Figure 7 displays tells us that, under the current model size, the

increasing relation between accuracy promotion and time consumption still keeps comparatively steady, hence the complete model still lies in a deployable reaction scope. If the model is used solely as a static classifier, the aforementioned improvements are insufficient to directly support on-site supervision; therefore, it is also necessary to observe the temporal evolution of the warning object, as shown in Figure 8.

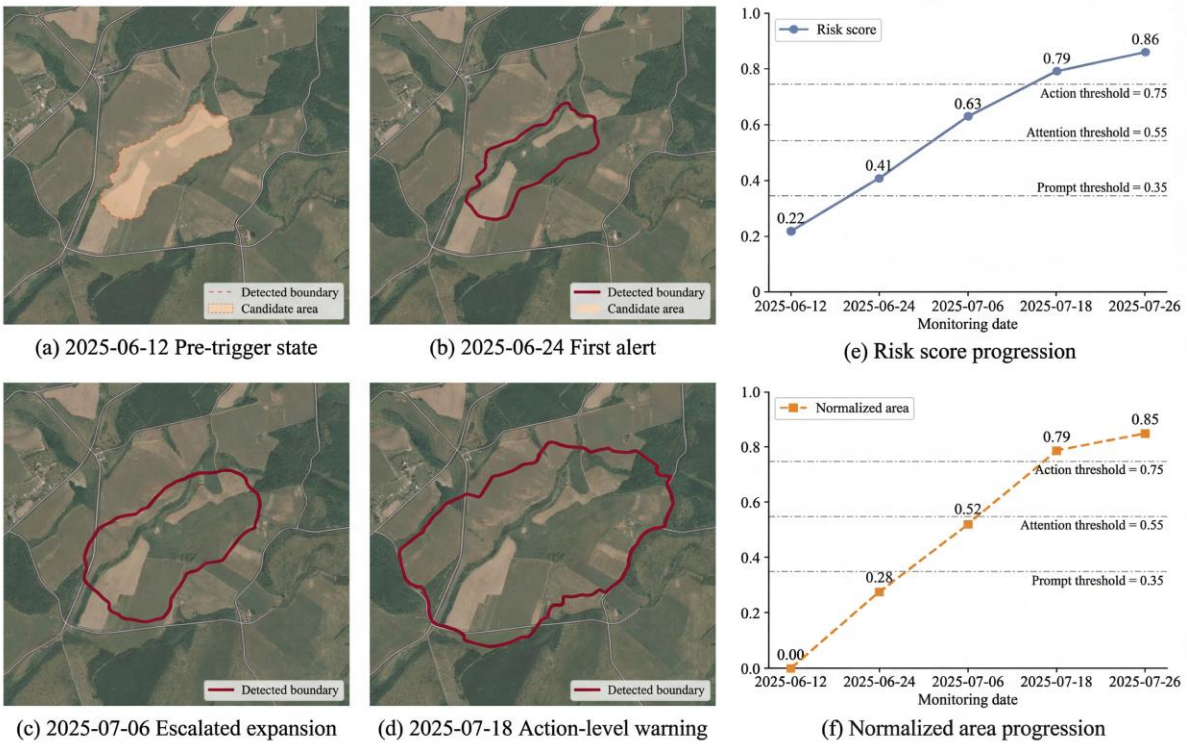

Figure 8: Temporal evolution of a warning object and risk score progression.

From Figure 8(a) to Figure 8(d), they give detection outcomes of the identical location on four different time points. On the day of 2025-06-12, any triggerable object had not yet formed; Up to the date 2025-06-24, one abnormal border has been firstly found out, which it covers a region of 426 square meters; Upon the date of 2025-07-06, it has been expanded to an area of 774 m²; and up to 2025-07-18, it got a further rise to 1184 m², whose boundary has a very clear expansion toward the outside. Figure 8(e) displays the alterations of risk scores and normalized area along with the passing of time. The risk values of score are 0.22, 0.41, 0.63, 0.79, and 0.86, separately; The values which get normalized by area are 0.00, 0.28, 0.52, 0.79, and 0.85, in order respectively. This system possesses three threshold lines, which are Prompt, Attention, and Action, their setting values are 0.35, 0.55, and 0.75, respectively. It can be observed that the system has passed the prompt threshold on 2025-06-24, passed the attention threshold on 2025-07-06, passed the action threshold on 2025-07-18, and therefore entered the on-site verification stage on 2025-07-26. What is more important, at the first two key nodes, the risk score values were 0.13 and 0.11 higher than the values after area normalization, respectively. This shows that early warning starting points do not only depend on region enlargement but are pushed by a mixed combination of lasting existence, departure from lawfulness, and environment sensitivity. This earlier rising of the risk reaction permits the system to put out intervention warnings before the target arrives at its biggest region.

Figures 7 and 8 collectively demonstrate that the improvements in this method are not isolated from one another. Temporal cues first determine whether a candidate anomaly proceeds to detailed investigation, geometric validity constraints are responsible for suppressing false

positives caused by highly similar backgrounds, and the boundary refinement head ensures better traceability of object-level area and boundaries during multi-temporal comparisons.

3.3 Visualization and Analysis

Although the whole outcomes have proven good accuracy and strong stability, the system may still meet mistakes in actual-world applications because of complicated backgrounds, lack of data, and size restrictions. In this section, we discuss the weaknesses of current system and directions for future improvements on basis of typical failure cases, as is shown in Figure 9.

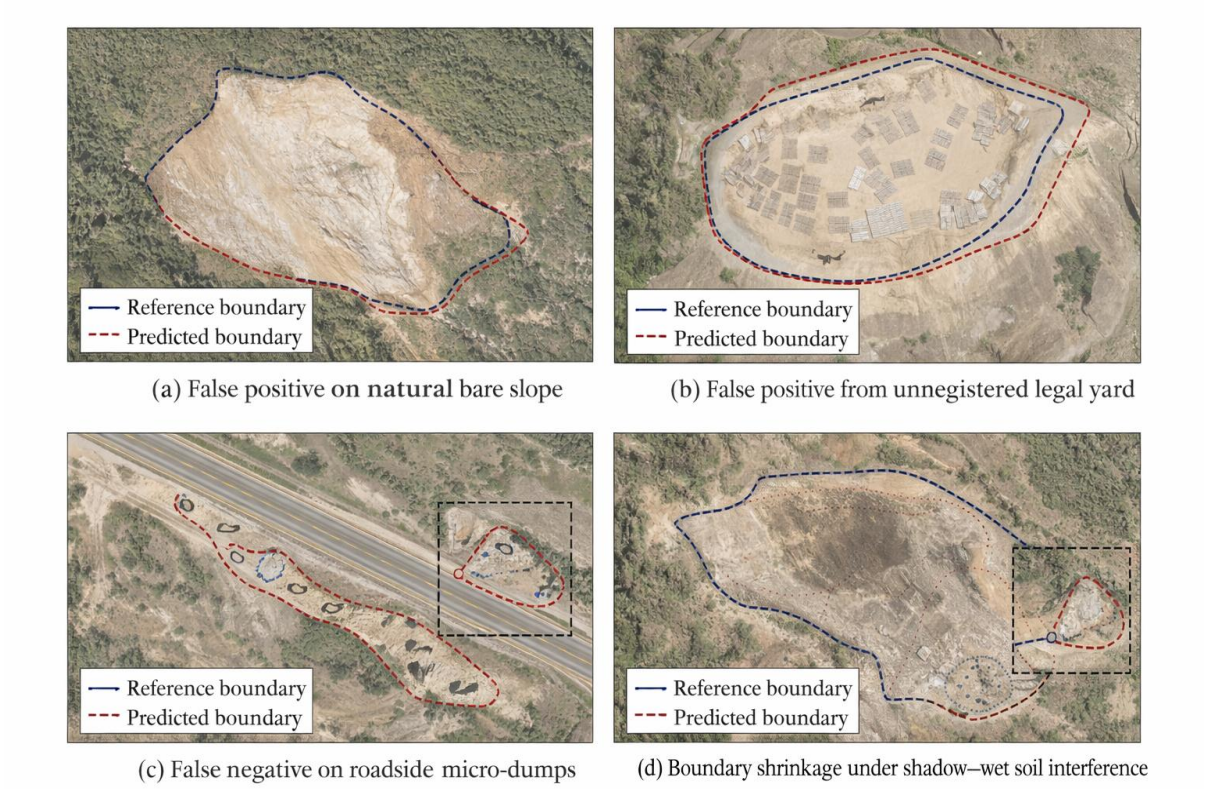

Figure 9: Typical false-positive and false-negative cases of CSBR-Net.

Figure 9(a) gives demonstration of one false-positive instance which relates to a natural bare slope. Even if this zone is not a designated place for throwing waste, its highly reflected exposed structure, closed outer shape, and slope expanding rule are very similar to those of unlawful waste throw, therefore it makes the model produce an overlarge forecasted boundary. Figure 9(b) shows us a false-positive example that includes a lawful stock which has not yet been put into the data bank. The dashed forecast outline on the whole superposes with the real stockpile region, hence showing that the classification based on image itself does not have obvious deviation; This problem, the main source is that external examination approval information has not been synchronized into this system. By contrast, the Figure 9(c) and Figure 9(d) are what express the situations of the detection that is missed. In Figure 9(c), merely the central part of a small, dispersed heap of rubbish by the road was detected, therefore it shows that the existing model still has not enough sensitivity for extremely small-sized, low-contrast objects; In Figure 9(d), the mixed background which is composed of shadows and wet soil caused that the predicted boundary contracts toward the inside, and the outer disturbance zone has not obtained complete restoration, therefore, this indicates that the overlapping of wet surfaces and shadows still brings interference to the learning of boundary.

As shown in Figure 9, errors at this stage primarily stem from four sources. The first is spectral interference between natural bare slopes, construction-exposed areas, and waste piles, a problem directly related to surface texture similarity; the second is incomplete metadata for authorized disposal sites and temporary storage areas, which weakens the effectiveness of geometric validity constraints;the third is the excessively small scale of small patches and scattered targets along roadsides, resulting in information loss between candidate screening and high-resolution verification; the fourth is boundary degradation caused by the superposition of shadows, wet soil, and local occlusions.The corresponding improvement strategies are also clear: First, records of approved disposal sites, temporary storage areas, and construction changes should be synchronized with the monitoring system in real time; second, the dataset should be expanded to include challenging samples from roadside edges, small scattered piles, and wet soil backgrounds; third, subsequent models should further enhance shadow suppression and surface moisture state constraints to reduce the probability of boundary shrinkage and target omission.

From an engineering application perspective, the aforementioned errors do not negate the system's practical value. For regulatory oversight around power construction projects, the system's primary task is to rapidly narrow down a large spatial area to a finite set of high-risk objects, and then prioritize these objects based on temporal evolution and spatial sensitivity. Current results indicate that CSBR-Net is already capable of providing relatively stable object-level screening results in complex bare-ground settings and establishing disposal priorities through the evolution of risk scores.

4 Conclusion

This article discusses the problems of "slow detection, hard distinction, and late early alert" in the supervision of unlawful dumping of construction waste and broken materials around power construction places through setting up a remote sensing monitoring frame which covers candidate area restrictions, target recognition, and object-level risk early warning. The outcomes prove that the system keeps comparatively stable recognition abilities under complicated bare-earth backgrounds and various engineering situations, and changes single-example recognition outcomes into continuous early alert information which can be utilized for on-spot checking and precedence arrangement.

(1) In the aspect of data arrangement, this research has built a multi-source observation system which is specially made for engineering supervision situations. Through bringing power line corridors, tower foundations, substation expansion zones, construction access roads, approved disposal sites, and high-resolution remote sensing imagery into a single candidate search region, the system raises spatial consistency between target search and legality evaluation.

(2) On the level of method and outcome, the CSBR-Net we put forward combines unusual time checking, legal shape limits, and edge adjustment into one identification flow, hence obtaining a highest F1 score of 89.2%, a mean F1 score of 89.6% in all situations, and a whole-model delay of 43.0 ms per image; At the same time, in the majority of instances, risk scores will increase prior to the occurrence of obvious area expansion, which shows that the framework has relatively good early warning prediction ability.

(3) The current system is still affected by factors such as the completeness of legal site metadata, small-scale scattered targets, and mixed backgrounds of shadows and wet soil. Future work could focus on dynamically updating approval layers, supplementing difficult samples of small targets, suppressing multi-temporal shadows, and conducting regional transfer validation to further enhance the system's applicability in real-world power construction supervision

environments.

Funding

This work was supported by State Grid Jibei Electric Power Co., Ltd. (52018K25000K).

About the Author

Zilong Zhou was born in June 1983 in Xuancheng, Anhui Province, China. He received his M.S. in Environmental Engineering from the University of Science and Technology Beijing, Beijing, China, in 2008. He is currently a Senior Engineer at the Low-Carbon and Environmental Protection Research Institute, Jibei Electric Power Research Institute, State Grid Jibei Electric Power Co., Ltd. His research interests include environmental protection in the power grid sector.

Tingming Ye gave birth in January 1995 at Wenzhou, which is in Zhejiang Province, China. He has obtained his degree of Ph. D. the degree of doctor in environmental engineering was obtained by me from the University of the Chinese Academy of Sciences which locates in Beijing, China, in the year of 2024. He at present holds the position of Engineer in the Low-Carbon and Environmental Protection Research Institute, Jibei Electric Power Research Institute, of State Grid Jibei Electric Power Co., Company Limited The directions of his research work contain the environmental protection work inside the power grid domain.

Wenliang Lin was born in January 1983 in Yantai, Shandong Province, China. He received his B.S. in Computer Science and Technology from North China Electric Power University, Beijing, China, in 2005. He is currently a Senior Engineer in the Construction Department at Zhangjiakou Power Supply Company, State Grid Jibei Electric Power Co., Ltd. His research interests include environmental and water protection management for power transmission and transformation projects.

References

[1] Sun, X., Liu, F., Zhao, Y., et al. (2024). Research on environmental risk monitoring and advance warning technologies of power transmission and distribution projects construction phase. Sensors, 24(23), 7695.

[2] Hu, X., Xia, B., Guo, Y., et al. (2025). Comprehensive monitoring of construction spoil disposal areas in high-speed railways utilizing integrated 3S techniques. Applied Sciences, 15(2), 762.

[3] Fraternali, P., Morandini, L., & González, S. L. H. (2024). Solid waste detection, monitoring and mapping in remote sensing images: A survey. Waste Management, 189, 88-102.

[4] Papale, L. G., Guerrisi, G., De Santis, D., et al. (2023). Satellite data potentialities in solid waste landfill monitoring: Review and case studies. Sensors, 23(8), 3917.

[5] Wang, B., Xing, Y., Wang, N., et al. (2024). Monitoring waste from uncrewed aerial vehicles and satellite imagery using deep learning techniques: A review. IEEE Journal of Selected Topics in Applied Earth Observations and Remote Sensing, 17, 20064-20079.

[6] Sun, X., Yin, D., Qin, F., et al. (2023). Revealing influencing factors on global waste distribution via deep-learning based dumpsite detection from satellite imagery. Nature Communications, 14(1), 1444.

[7] Torres, R. N., & Fraternali, P. (2023). AerialWaste dataset for landfill discovery in aerial and satellite images. Scientific Data, 10(1), 63.

[8] Lin, S., Huang, L., Liu, X., et al. (2024). A construction waste landfill dataset of two districts in Beijing, China from high resolution satellite images. Scientific Data, 11, 388.

[9] Yong, Q., Wu, H., Wang, J., et al. (2023). Automatic identification of illegal construction and demolition waste landfills: A computer vision approach. Waste Management, 172, 267-277.

[10] Sánchez-Fernández, M., Arenas-García, L., & Gutiérrez Gallego, J. A. (2023). Detection of construction and demolition illegal waste using photointerpretation of DEM models of LiDAR data. Land, 12(12), 2119.

[11] Zhang, S., & Ma, J. (2024). CascadeDumpNet: Enhancing open dumpsite detection through deep learning and AutoML integrated dual-stage approach using high-resolution satellite imagery. Remote Sensing of Environment, 313, 114349.

[12] Gibellini, F., Fraternali, P., Boracchi, G., et al. (2025). A deep learning pipeline for solid waste detection in remote sensing images. Waste Management Bulletin, 3(4), 100246.

[13] Yu, J., Mao, P., Wu, W., et al. (2025). TSNET: A solid waste instance segmentation model in China based on a two-step detection strategy and satellite remote sensing images. International Journal of Applied Earth Observation and Geoinformation, 136, 104366.

[14] Berra, E. F., Fontana, D. C., Yin, F., et al. (2024). Harmonized Landsat and Sentinel-2 data with Google Earth Engine. Remote Sensing, 16(15), 2695.

[15] Li, Y., & Zhang, X. (2024). Multi-scale context fusion network for urban solid waste detection in remote sensing images. Remote Sensing, 16(19), 3595.

[16] Zhou, L., Rao, X., Li, Y., et al. (2023). SWDet: Anchor-based object detector for solid waste detection in aerial images. IEEE Journal of Selected Topics in Applied Earth Observations and Remote Sensing, 16, 306-320.

[17] Li, H., Hu, C., Zhong, X., et al. (2023). Solid waste detection in cities using remote sensing imagery based on a location-guided key point network with multiple enhancements. IEEE Journal of Selected Topics in Applied Earth Observations and Remote Sensing, 16, 191-201.

[18] Torres, R. N., & Fraternali, P. (2021). Learning to identify illegal landfills through scene classification in aerial images. Remote Sensing, 13(22), 4520.

[19] Bai, T., Wang, L., Yin, D., et al. (2023). Deep learning for change detection in remote sensing: A review. Geo-spatial Information Science, 26(3), 262-288.

[20] Chen, H., & Shi, Z. (2020). A spatial-temporal attention-based method and a new dataset

for remote sensing image change detection. Remote Sensing, 12(10), 1662.

[21] Chen, H., Qi, Z., & Shi, Z. (2021). Remote sensing image change detection with transformers. IEEE Transactions on Geoscience and Remote Sensing, 60, 1-14.

[22] Lu, K., Huang, X., Xia, R., et al. (2024). Cross attention is all you need: Relational remote sensing change detection with transformer. GIScience & Remote Sensing, 61(1), 2380126.

[23] Wang, D., Zhang, J., Du, B., et al. (2023). An empirical study of remote sensing pretraining. IEEE Transactions on Geoscience and Remote Sensing, 61, 1-20.

[24] Bastani, F., Wolters, P., Gupta, R., et al. (2023). SatlasPretrain: A large-scale dataset for remote sensing image understanding. In 2023 IEEE/CVF International Conference on Computer Vision (pp. 16726-16736).

[25] Padubidri, C., Kamilaris, A., & Karatsiolis, S. (2022). Accurate detection of illegal dumping sites using high resolution aerial photography and deep learning. In 2022 IEEE International Conference on Pervasive Computing and Communications Workshops and Other Affiliated Events (pp. 451-456).